TEVATRON STUDY REPORT: PBAR TUNES & PBAR REMOVAL 11/17/02

V. Shiltsev, X.L. Zhang, F. Zimmermann*

Abstract

In the end-of-the-store study on November 17, 2002, we excited individual pbar bunches using the Tevatron Electron Lens (TEL) and detected the associated signals in the proton and pbar vertical Schottky spectra, as well as their response to pbar and proton tune changes The tune for the p-bar bunch A24 could thus be inferred. Subsequently, the antiprotons were slowly scraped to nearly zero intensity, in an attempt to compare the p-bar emittances obtained by the flying wires and by the synchrotron light monitor with those derived from the remaining beam intensity measured as a function of collimator position.

1 SEQUENCE OF EVENTS

Pbar tune measurements were conducted from 16:10 to 18:50. From 18:51 to 20:00 we scraped the antiproton beam.

We set up the TEL, such that it operated in a short burst. White noise was added, which modulated the electron current on each turn. Inspecting the bunches whose intensity was reduced, we concluded that we first excited A36, next A1, and then A5. Still on A5, we scanned the pbar vertical Schottky power versus the noise voltage. The result is illustrated in Fig. 1, which demonstrates that we indeed excited the beam.

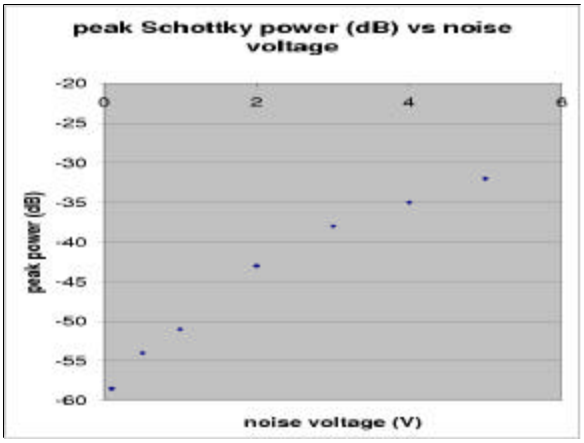

Figure 1: Vertical pbar Schottky peak power as a function of TEL noise voltage.

Note that the vertical pbar Schottky monitor had recently been adjusted for optimum suppression of the proton signal, and a suppression factor of 10 dB had been demonstrated (expected ideal suppression is 20 dB). A similar optimisation for the horizontal monitor had not yet been performed.

In the following, we varied the horizontal TEL position from 0 to –5 mm (the setting of the 1st TEL corrector changed from –27 to –195). At –3 mm (corrector setting –126) the pbar losses went up. We assumed that this was close to the pbar beam position, in agreement with its expected value. We left the electron beam at this position. The evolution of the proton and pbar Schottky power, and the pbar loss rate, during the horizontal position scan is shown in Fig. 2.

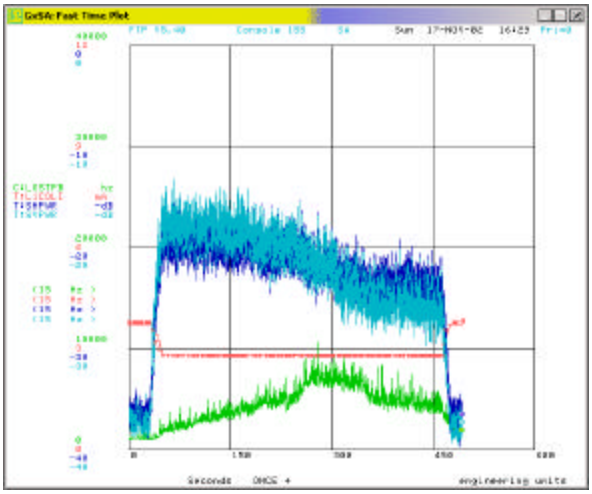

Figure 2: Evolution of Schottky power (the signal labelled SHPWR is pbar vertical!) as the electron beam is moved by –5 mm horizontally across the pbar beam. A bump in the pbar losses occurred at –3 mm, where the electrons are thought to be nearest to the pbars. For large negative displacement the pbar Schottky power exceeds that of the protons, which continually decreases towards the right.

Next, we adjusted the TEL timing, and centred the TEL current signal on the pbar bunch A12. Note here that the bunches at the end of a train are special, since it is possible to excite them by the TEL without affecting the proton beam. For all other antiproton bunches, a proton bunch arrives nearly simultaneously (though horizontally separated). This is due to the location of the TEL along the ring, i.e., its distance to the main interaction points, and to the 396-ns bunch spacing of Run-IIa.

For a noise-voltage of 4 V, the TEL peak current extended over a range of 150-250 mA, so that the peak-to-peak modulation amplitude amounted to 50%. We recorded Schottky data for bunch A12. When we noted that this bunch had almost disappeared (the TEL excitation had shortened the bunch lifetime to less than 20 minutes), we switched to A24 (at 18:08), and lowered the noise voltage from 4 V to 2 V.

*visiting from CERN

For A 24 we took Schottky data with and without the TEL excitation, and observed the changes when moving the horizontal antiproton tune up by 0.002, the vertical antiproton tune down by –0.002, and the vertical proton tune also down by –0.002. This test confirmed our identification of the pbar tunes in the Schottky spectrum.
To scrape the antiproton beam, we followed a procedure recommended by D. Still, and moved a set of six (horizontal and vertical) collimators simultaneously towards the beam until the intensity FBIANG indicated zero current. In this condition, turning on and off the TEL no longer had an effect on the Schottky spectrum, except for a short transient.
We finally measured the chromaticity of the proton beam in the collision optics at 980 GeV, varying the rf frequency by only +/- 10Hz, and obtained the values Ch~13, Cv~16.
Despite of the smallness of the rf frequency change, this measurement had generated a significant amount of coasting beam, at each of the three frequency steps (why?). We tried to remove this dc component using the normal TEL excitation set up for dc-beam removal, but the improvement was slow, with a time constant on the order of several hours. After waiting for about 30 minutes only, the beam was dumped, resulting in a quench.

2 PBAR TUNE MEASUREMENT

Figures 3 and 4 show the vertical Schottky spectra for protons and antiprotons, when the TEL was turned off or on, respectively.

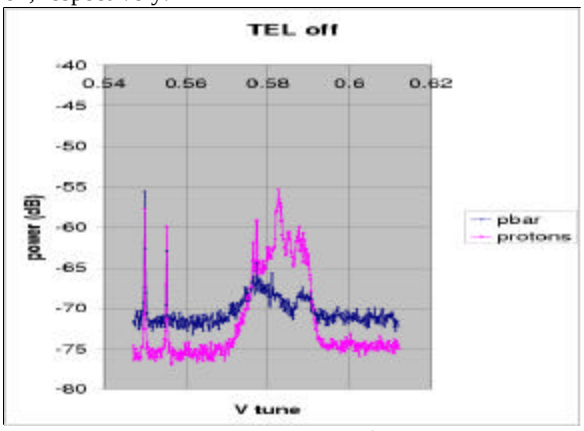

Figure 3: Vertical Schottky spectra for protons and pbars without TEL excitation.

Here and in the following the TEL excited bunch A24. Without TEL the pbar signal is 10 dB lower than the proton signal, in accordance with the previously measured suppression factor between the two channels. When the TEL is on, the pbar spectrum is higher by about 7-10 dB over most of the frequency range. In particular, the peaks in the pbar spectrum are now higher than those in the proton spectrum. The smaller peak on the left is believed to be the vertical tune. For both protons and pbars, the right peak in the spectrum is the horizontal tune.

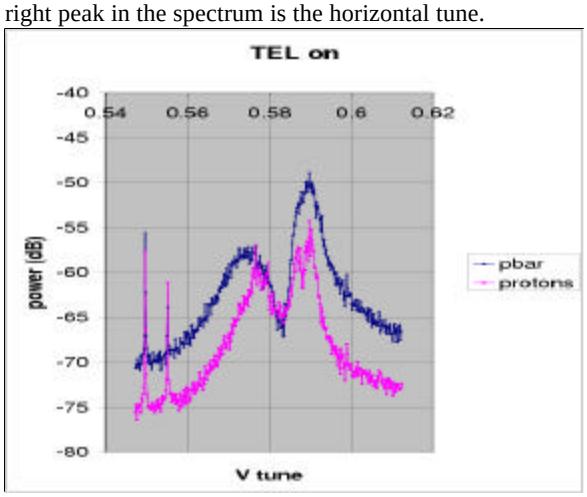

Figure 4: Vertical Schottky spectra for protons and pbars with TEL excitation of pbar bunch A24.

Figures 5 and 6 illustrate the change in the pbar and proton spectrum, respectively, that occurred, when the horizontal pbar tune was increased by +0.002, and afterwards set back to its original value. In the pbar spectrum, the purple line is shifted upwards by about the expected amount, while the positions of the peaks in the proton spectrum exhibit no noticeable change

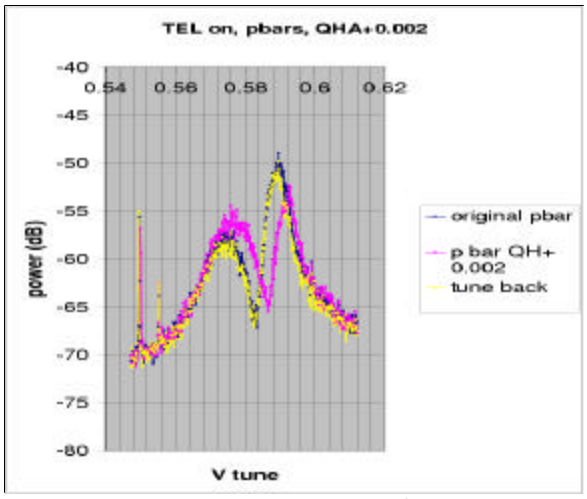

Figure 5: Vertical Schottky spectra of pbars with TEL excitation of pbar bunch A24, showing the effect of a pbar horizontal tune change by +0.002 and subsequent reset.

Figures 7 and 8 display the effect of changing the vertical proton tune by a nominal value of -0.002. In Fig. 7, the pbar spectrum is unchanged, but, in Fig. 8, the left peak in the proton spectrum moves downwards (though somewhat less than expected).

The following two figures, 9 and 10, illustrate the effect of lowering instead the pbar vertical tune by –0.002.

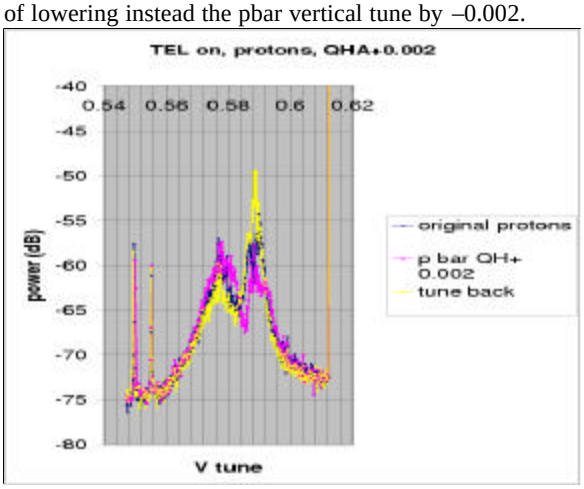

Figure 6: Vertical Schottky spectra of protons with TEL excitation of pbar bunch A24, showing the effect of a pbar horizontal tune change by +0.002 and subsequent reset

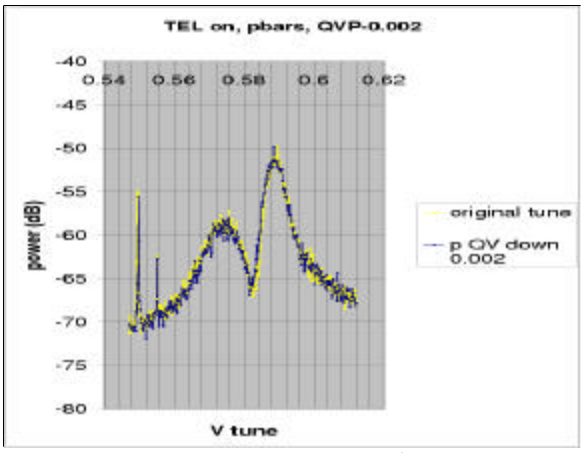

Figure 7: Vertical Schottky spectra of pbars with TEL excitation of pbar bunch A24, showing the effect of a proton vertical tune change by –0.002 and subsequent reset.

We observe a small downward shift of the left peak in the pbar spectrum, and no obvious effect on the proton signal.

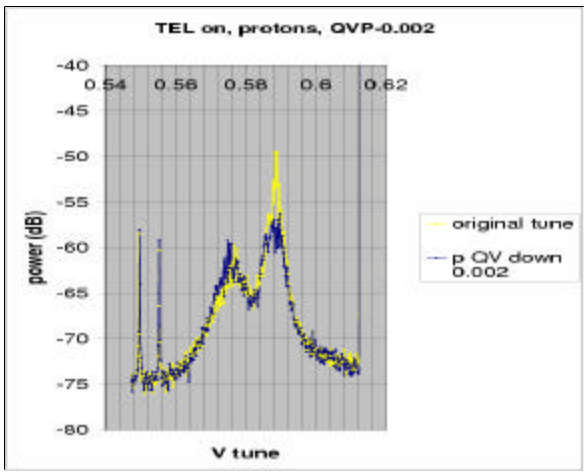

Figure 8: Vertical Schottky spectra of protons with TEL excitation of pbar bunch A24, showing the effect of a proton vertical tune change by +0.002 and subsequent reset

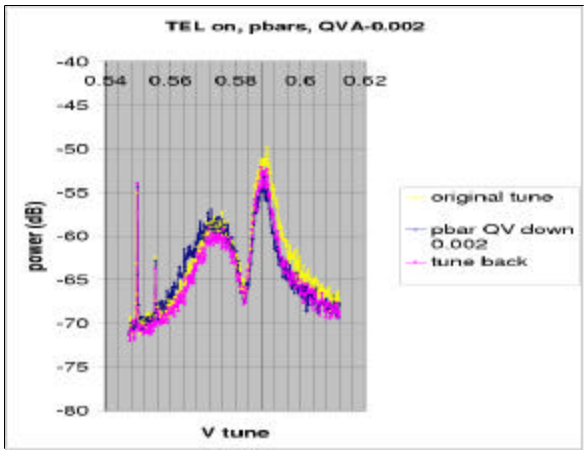

Figure 9: Vertical Schottky spectra of pbars with TEL excitation of pbar bunch A24, showing the effect of a pbar vertical tune change by –0.002 and subsequent reset.

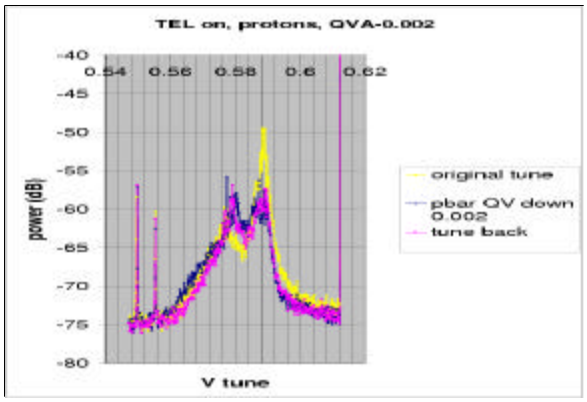

Figure 10: Vertical Schottky spectra of protons with TEL excitation of pbar bunch A24, showing the effect of a pbar vertical tune change by –0.002 and subsequent reset.

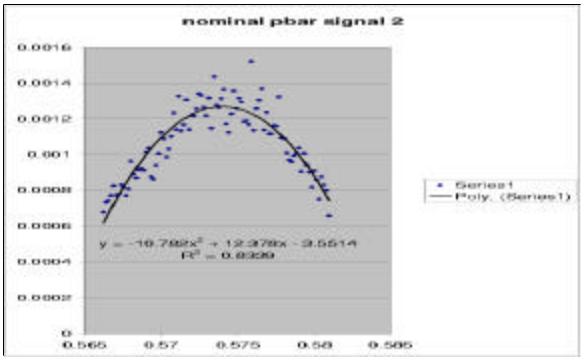

Figure 11: Inverse parabola fitted to linear pbar Schottky spectrum around the lower peak (vertical tune) for nominal quadrupole setting.

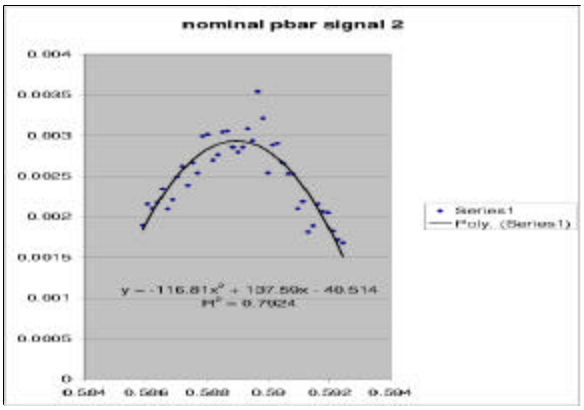

Figure 12: Inverse parabola fitted to linear pbar Schottky spectrum around the upper peak (horizontal tune) for nominal quadrupole setting.

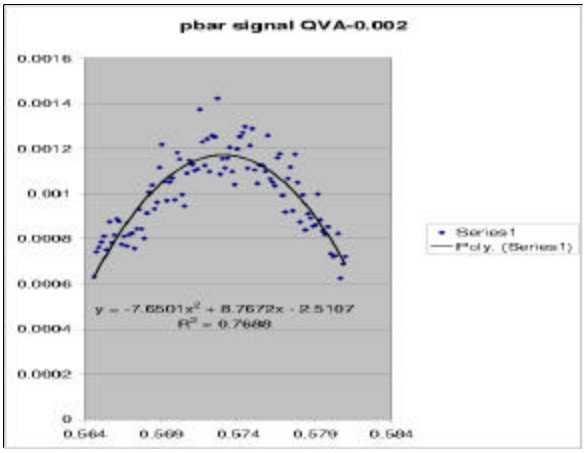

Figure 13: Inverse parabola fitted to linear pbar Schottky spectrum around the lower peak (vertical tune) for a change in the vertical pbar tune by –0.002.

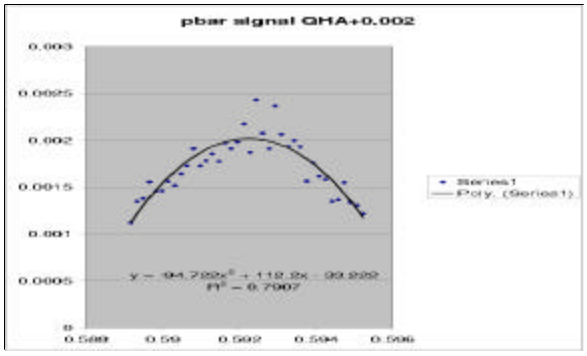

Figure 14: Inverse parabola fitted to linear pbar Schottky spectrum around the upper peak (horizontal tune) for a change in the horizontal pbar tune by +0.002.

To obtain a better resolution on the pbar tune we fitted the vicinity of each peak on a linear scale to an inverse parabola. Fit examples are shown in Figs. 11-14.
If the fitted parabola is of the form $Q = ax^2 + bx + c$, the tune is taken to be the value at the maximum, or $Q_0 = -b/(2a)$. For the protons, the inverse parabola does not give a good fit, and we simply took the peak of the tune line, which in this case is much narrower, presumably due to the much reduced beam-beam tune spread of the protons. The tune values for protons and pbars obtained in this way are summarized in Table 1. (Note that the value for the horizontal proton tune was modified compared with that quoted in a preliminary analysis, where we took the peak of Fig. 3 as the unperturbed proton tune, which was not reproduced in any of the later measurements and apparently was a 'ghost line'.)

Table 1: Horizontal and vertical tunes of the antiproton bunch A24 and of the protons.

	QH	QV
pbar	0.5897+/-0.0003	0.5741+/-0.0002
Protons	0.5888+/-0.003	0.5770+/-0.0003

The vertical tune of pbar bunch 24 is about 0.003 lower than the vertical proton tune, the horizontal tune of A24 is about 0.001 higher than the corresponding proton tune. When changing the horizontal pbar tune by +0.002, we measured an upward shift in the with peak of 0.0026+/-0.0004. For the vertical pbar tune change of –0.002, the left peak in the pbar spectrum moved by about -0.0013+/-0.0004.
In the subsequent scraping experiment we had the opportunity to take vertical Schottky spectra with and without pbars. This comparison is depicted in Figs. 15 and 16. The proton Schottky spectrum is virtually unchanged, when the pbars are removed, whereas the left peak in the pbar spectrum decreases. Therefore, this peak appears to have been the vertical proton tune, here visible even without TEL excitation. The right peak in the

vertical pbar spectrum (again without TEL excitation) is attributed to the proton beam, since it is still present after the pbar removal. This signal is at least 10 dB lower (and at a different tune) than the horizontal pbar tune we had identified earlier with the TEL being active.

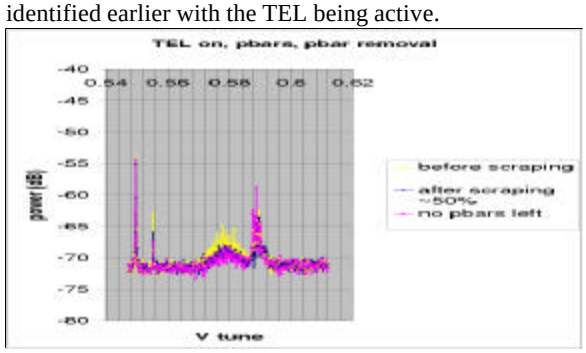

Figure 15: Vertical Schottky spectra of pbars with TEL excitation of pbar bunch A24, illustrating the effect of pbar removal.

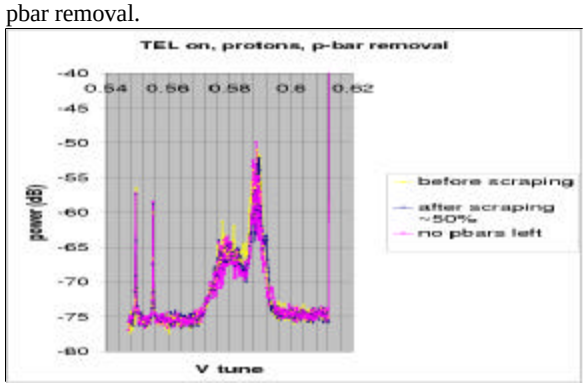

Figure 16: Vertical Schottky spectra of protons with TEL excitation of pbar bunch A24, illustrating the effect of pbar removal.

3 PBAR REMOVAL

In the second part of the MD, the antiprotons were removed following a procedure suggested by D. Still. Six collimator jaws were employed with the following names and relevant optical functions (computed by MAD):

(1) F49H, β_x=207 m, D_x=3.24 m,
(2) F49V, β_y=43 m,
(3) F48H, β_x=112 m, D_x=2.26 m,
(4) F48V, β_y=28 m,
(5) D172H, β_x=66 m, D_x=4.254 m,
(6) D172V, β_y=49 m.

The first two collimators are believed to do most of the scraping in the horizontal (and momentum) plane and in the vertical plane, respectively. The collimator step size is 1 mil, equal to 0.025 mm. Figure 17 shows the total pbar intensity, recorded by C:FBIANG as a function of the step position of collimator F49H.

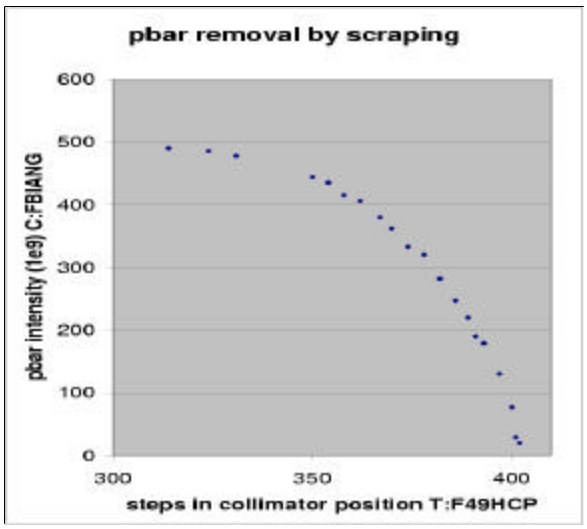

Figure 17: Total stored pbar intensity as a function of the horizontal collimator position F49H in units of steps.

Figure 18 provides some background information, which will help to understand the following results for the antiprotons. Namely, this figure again shows the collimator position, together with the proton bunch length and proton intensity during the period of the pbar scraping. The protons were not scraped, but their intensity dropped about 15 min. after the pbar removal had been completed (the latter lasted from 19.5 to 19.8 hr) by roughly $2x10^{11}$, or 10%, as a result of the proton chromaticity measurement. At the same time, the proton bunch length increased by about 0.1-0.2 ns.

Figure 19 shows the reduction in pbar intensity as seen by different detectors. In principle, the readings from SBDAIS, FBIANG, and the difference between total and proton current, (TIBEAM-FBIPNG), should all give the same number. At the start of the removal, SBDAIS and FBIPNG are identical, but between 19.8 and 19.9 hr FBIPNG drecreases to zero, after the scraping, while SBDAIS remains at a nonzero value equal to about 10% of the initial intensity. The difference of TIBEAM (sum of proton and pbar currents) and the proton intensity FBIPNG initially is about 20% higher than the other two pbar intensity readings. This difference increases during the pbar removal, and it even makes a step upwards at the moment of the proton chromaticity measurement, where protons were lost and the proton bunch length increased.

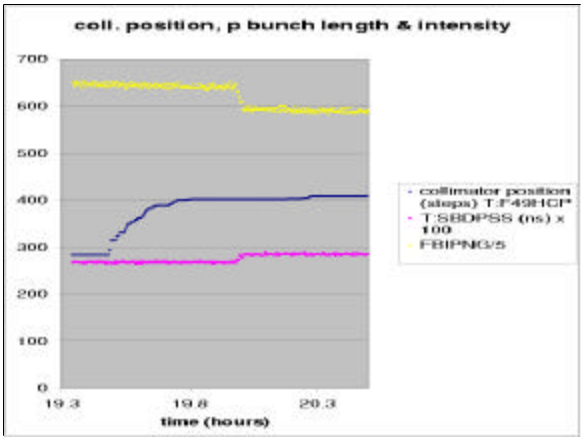

Figure 18: The horizont al collimator position F49H in units of steps, the rms proton bunch length (in 0.01 ns), and the total proton intensity (in $2x10^8$) as a function of time in hours during the removal.

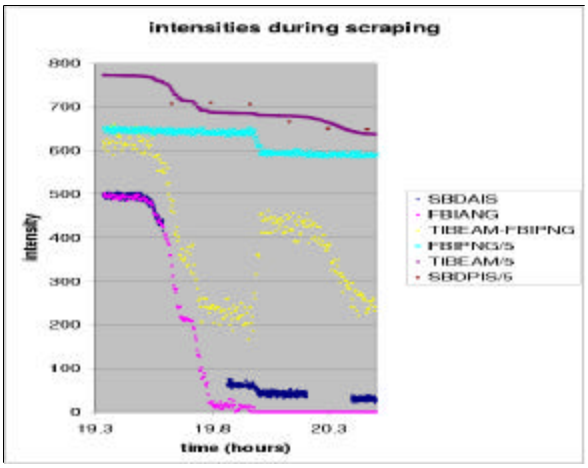

Figure 19: The horizontal collimator position F49H in units of steps, the pbar intensity from SBD and from FBIANG, both in units of 10^9, the difference between IBEAM and FBIPNG (which should also equal the pbar intensity) in 10^9, the proton intensity (in $2x10^8$), and the total beam intensity (in $2x10^8$) as a function of time in hours during the pbar removal.

Since a circumstantial evidence suggests that a non-negligible number of pbars were still present after the scraping (see below), the SBDAIS reading appears to be the most plausible.

Centroid positions and beam sizes from the synchrotron light monitor, recorded during the same time span, are shown in Figs. 20-23 for four representative pbar bunches: A1, A5, A8, A24. Three of these had been excited by the TEL, and bunch no. 8 was thought to represent a non-affected typical bunch.

The beta functions at the light-monitor source point are β_x=49 m, β_y=108 m, and the dispersion D_x=1.92 m. The rms beam sizes are of the order of 0.5-1.0 mm. Hence, the centroid motion and the bunch-to-bunch differences in Figs. 20 and 21 are small, a few percent of the beam size at the most. Both transverse beam sizes decrease during the scraping, suggesting that either we collimated in both planes, as we might have anticipated, and/or that the coupling is significant.

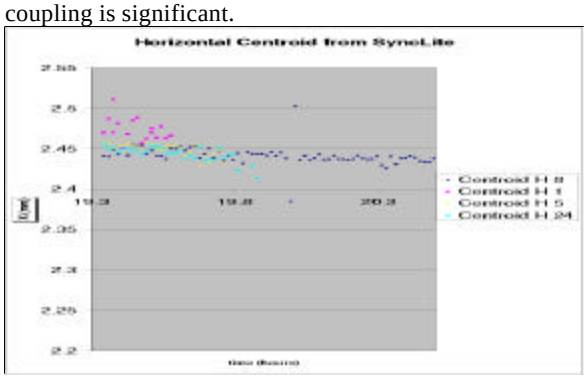

Figure 20: The horizontal centroid positions detected by the synchrotron light monitor for four different pbar bunches as a function of time in hr.

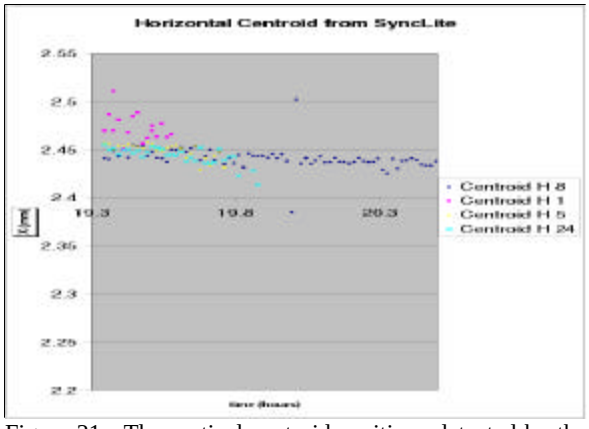

Figure 21: The vertical centroid positions detected by the synchrotron light monitor for four different pbar bunches as a function of time in hr.

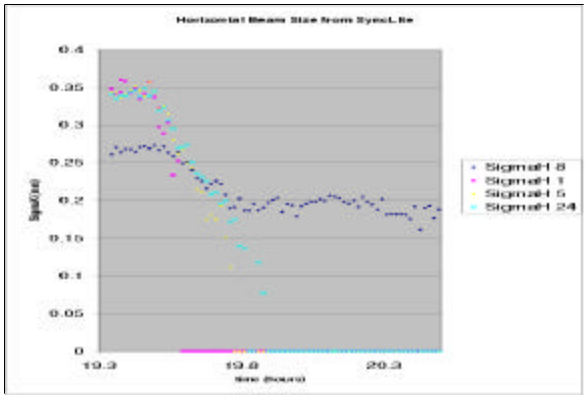

Figure 22: The horizontal beam size detected by the synchrotron light monitor for four different pbar bunches as a function of time in hr.

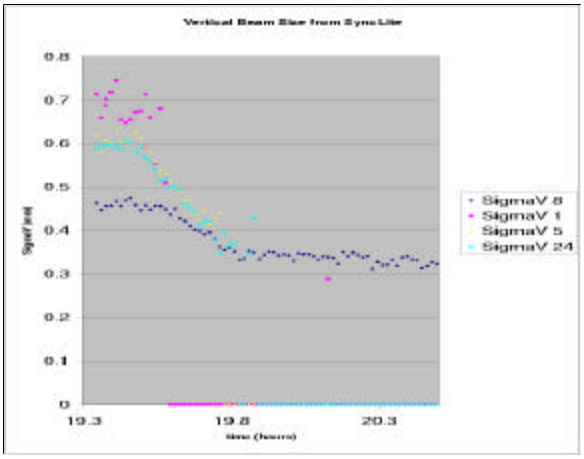

Figure 23: The vertical beam size detected by the synchrotron light monitor for four different pbar bunches as a function of time in hr.

Figures 24 and 25 display the corresponding emittances obtained from the synchrotron light beam sizes. The result for our nominal bunch 8 is surprising. While the emittances of all excited bunches went to zero, in Fig. 24, the horizontal emittance of bunch 8 increased and, in Fig. 25, the vertical stayed almost constant. The horizontal beam size, in Fig. 22, did not increase, however. The apparent discrepancy may indicate a correction algorithm, e.g., for the beam momentum spread, which fails at the reduced bunch intensity.

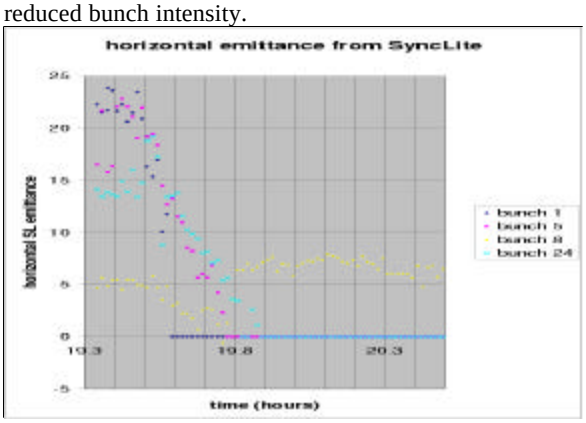

Figure 24: The horizontal emittance inferred from the synchrotron light monitor for four different pbar bunches as a function of time in hr.

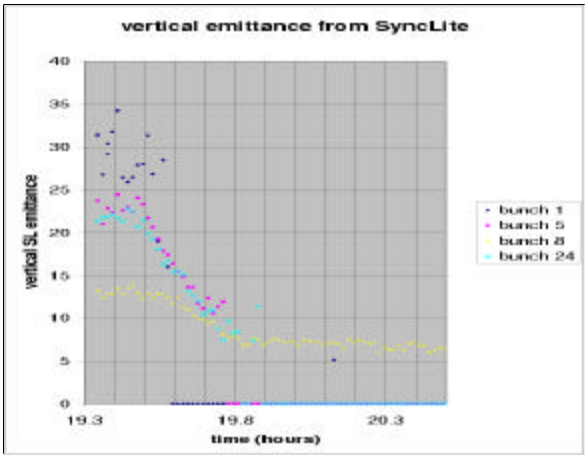

Figure 25: The vertical emittance inferred from the synchrotron light monitor for four different pbar bunches as a function of time in hr.

To cross-calibrate the synchrotron-light data, we have flown the wires several times during the pbar removal. Figures 26 and 27 show the resulting TevArray display with flying-wire emittances, bunch lengths, and bunch intensities for protons and pbars, respectively.

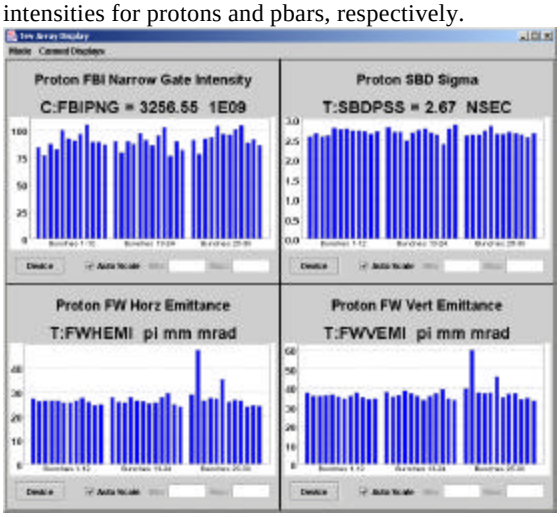

Figure 26: TevArray display with proton bunch intensities, bunch lengths, and emittances from flying wires measured prior to pbar removal.

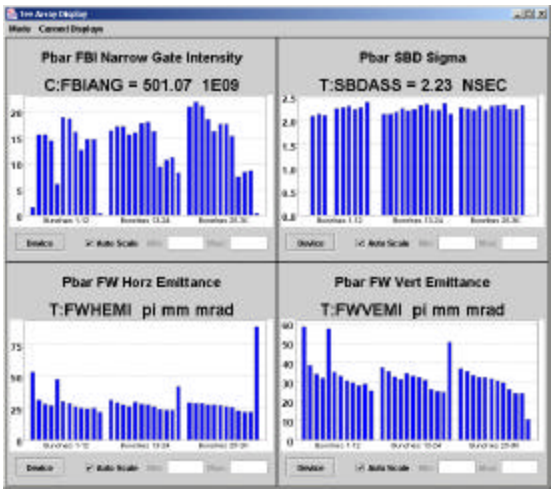

Figure 27: TevArray display with pbar bunch intensities, bunch lengths, and emittances from flying wires measured prior to pbar removal.

We tried to extract an independent measurement of the emittance from the beam loss during the scraping itself. The fraction of the beam which is lost depends on the collimation amplitude a as

$$f = \exp\left(-\frac{a^2}{2s^2}\right).$$

Thus by measuring the beam fraction which is lost, or, alternatively, the surviving part (1-f) and fitting to a Gaussian, we should be able to determine the rms beam size at the scraper. The amplitude a is defined with respect to center of the beam, which is precisely known only once the beam is completely removed. Another difficulty is that in our experiment several collimators were moved in parallel.

For example, F49H was moved by a total of 88 steps, while F49V was moved by about 36 steps. When evaluating the effect of these collimators on the beam distribution, we should then take into account that the vertical beta function is 4 to 5 times smaller and also that there is a nonzero horizontal dispersion at F49H. Accordingly, the simultaneous motion of these two collimators with the quoted ratio of step sizes may yield a similar scraping effect in all three degrees of freedom. In Figs. 24-25, we have seen that indeed both the horizontal and vertical beam sizes were reduced during the scraping. Unfortunately, only sparse and rather inconclusive longitudinal data from the SBD were available during the period of the scraping; they hinted at merely a small reduction in the bunch length.

For simplicity, in the following we first ignore these complications and assume that the scraping occurs in a single plane. Figure 28 displays the logarithm of the lost beam fraction as a function of the collimator position. The zero of the horizontal axis was adjusted to approximate a parabola with a maximum at zero. From the 2nd order polynomial fit, we infer an effective beam size of $s \approx 760\mu m$. Assuming a dispersion of 3.2 m, and an rms momentum spread of 1.15×10^{-4}, the expected rms beam size at the collimator F49H due to the dispersive component alone is $s_d \approx 373\,\mu m$. Subtracting this in quadrature from the fitted value of σ, the effective transverse beam size becomes $s_b \approx 662\,\mu m$. With a beta function of about 200 m, we obtain a $6\sigma^2$ normalized transverse emittance of 14 μm. Without subtracting the dispersive part, it would be 18 μm.

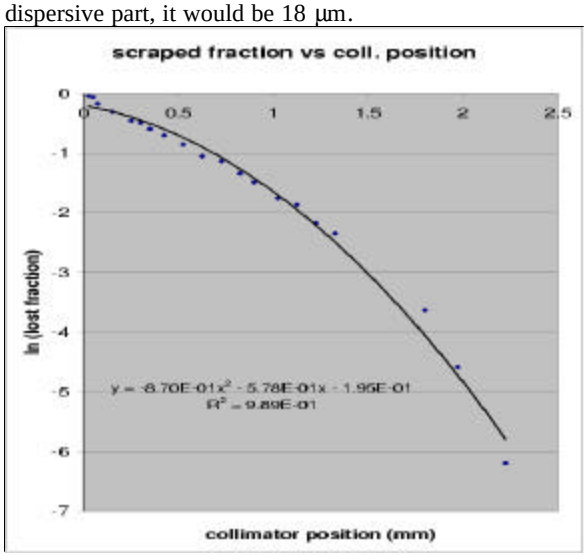

Figure 28: Natural logarithm of lost beam fraction (inferred from FBIANG) as a function of collimator position F49H, and a parabolic fit to the data. The horizontal zero was adjusted 'by eye' to give the best parabolic curve approaching zero at zero amplitude.

From the beam loss ΔN encountered for each step movement Δr of the collimator, we can also attempt to reconstruct the radial beam density ρ, using the relation

$$\Delta r \approx \frac{\Delta N}{2\pi r \Delta r}.$$

For a Gaussian profile the expected density function is

$$r_{\text{Gaussian}} = \frac{Ne^{-\frac{r^2}{2s^2}}}{2\pi r s^2},$$

where a factor r also enters in the denominator.The result of such a calculation is shown in Fig. 29. The curve at small amplitudes is sensitive to the exact position of zero. In this particular experiment the zero point was difficult to determine, since it varied depending on the current monitor. In addition, a significant number of pbars were apparently still present at the end of the study (seen both on the light monitor and on the wire scans). These could not be removed even by pushing the collimator further

inwards by several steps. We do not have a good explanation for this effect, but it might be attributed to the simultaneous collimation in three degrees of freedom in conjunction with a fragmented non-Gaussian beam distribution.

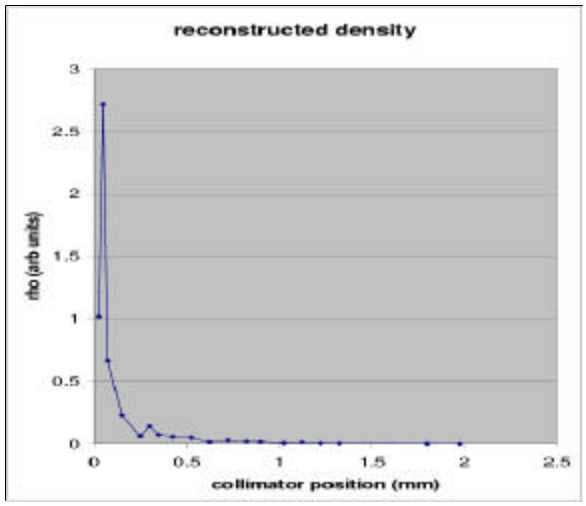

Figure 29: Radial beam density reconstructed from beam loss at each scraping step as a function of the radial distance from the origin.

We can now compare the emittances prior to scraping inferred from the synchrotron-light (SL) monitor, from the flying wires (FW), and from the amplitude-dependent intensity reduction during the pbar removal (scraping). All numbers are listed in Table 2. As before, three of the individual bunches listed (A1, A5, and A24) correspond to bunches blown up or almost eliminated by the TEL excitation; compare also the synchrotron-light beam sizes displayed in Fig. 30. In Table 2, it is noteworthy that the SL and FW emittances are different by about a factor of 2 throughout. The emittances inferred from the scraping lie somewhere in between. The latter two numbers were obtained by assuming that the scraping occurs either only horizontally at collimator F49H or only vertically at F49V. However, the beam-size measurements indicated that we scraped in both planes at the same time. If the the scarping efficiency for the two planes was about equal, the fraction of the beam lost as a function of collimator position would be given by the square of f in the above equation, and the real emittance would be two times larger than that inferred from the 1-dimensional parabolic fit. Considering this additional factor of two, the emittance numbers inferred from the scraping appear roughly consistent with those determined by the flying wire.

Table 2: Pbar horizontal and vertical 6σ normalized emittances prior to scraping, measured by three different methods.

horizontal	'typical'	A1	A5	A8	A24
FW	25	52	48	25	40
SL	5	24	22	5	14
scraping	14?	-	-	-	-
vertical	'typical'	A1	A5	A8	A24
FW	25	59	58	30	50
SL	12	30	23	12	21
scraping	22?	-	-	-	-

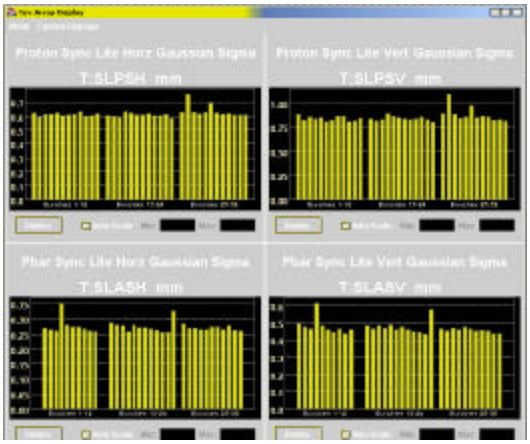

Figure 30: Proton (top) and pbar (bottom) synchrotron-light beam sizes prior to scraping. Bunch A1 is not visible (due to too low intensity?), bunches A5 and A24 are clearly blown up.

Table 3 shows the emittances from the synchrotron-light monitor and from the flying wire recorded after scraping 60% of the pbar intensity. There still remains an approximate factor of two discrepancy between the two detectors.

Table 4 lists the corresponding values for the end of the scraping, when, from the FBIPNG reading, we had expected that no pbars were left. However, both monitors still displayed updated emittance numbers for most of the pbar bunches.

Figure 31 illustrates the synchrotron-light beam-size summary display after the scraping. Wire scanner profiles before and after scraping are shown in Figs. 32 and 33 (unfortunately not for the same bunch). The beam profiles after scraping still have a nicely Gaussian shape (though narrower than in the beginning), which also suggests that there were still a significant number of pbars in the ring.

Table 3: Pbar horizontal and vertical 6σ normalized emittances after scraping 60% of the intensity, measured by the synchrotron-light monitor and the flying wires.

horizontal	'typical'	A1	A5	A8	A24
FW	15	-	14	15	14
SL	3?	-	6	3	8
vertical	'typical'	A1	A5	A8	A24
FW	18	6	21	18	18
SL	9?	-	11	9	11

Table 4: Pbar horizontal and vertical 6σ normalized emittances after the pbar scraping, measured by synchrotron-light monitor and flying wires.

horizontal	'typical'	A1	A5	A8	A24
FW	8	3	-	8	9
SL	7??	-	-	7	3
vertical	'typical'	A1	A5	A8	A24
FW	8	7	26	8	9
SL	7??	-	-	7	7

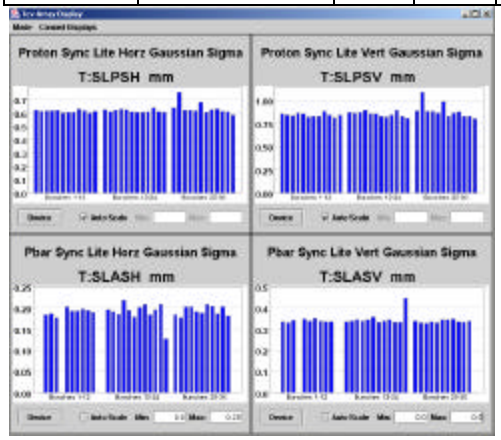

Figure 31: Proton (top) and pbar (bottom) synchrotron-light beam sizes after the pbar scraping. Bunches A1 and A5 are not visible (presumably due to the very low intensity), bunch A24 is blown up only vertically.

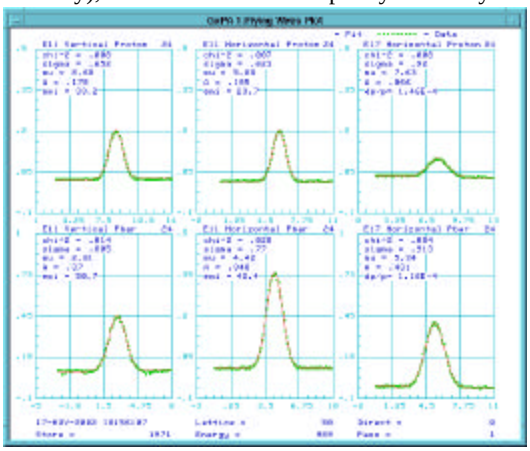

Figure 32:Proton (top) and pbar (bottom) flying-wire beam profile for bunches P24 and A24 before scraping.

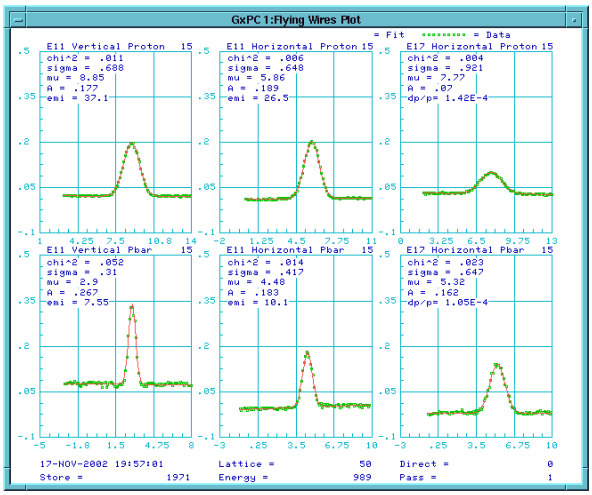

Figure 32: Proton (top) and pbar (bottom) flying-wire beam profile for bunches P15 and A15 after scraping.

4 CONCLUSIONS

We measured the pbar tunes at 980 GeV by exciting individual pbar bunches with the electron lens. The affected bunches blew up and lost intensity, at a rate depending on the noise modulation amplitude of the electron current. The tunes of pbar bunch A24 were found to be about 0.003 lower vertically and 0.001 higher horizontally than the average proton tune.

It is interesting that independent calculations by D. Shatilov, Y. Alexahin, T. Sen, and (first, but for a different optics [1]) P. Bagley predict that all bunches in a train have roughly the same tune except for the horizontal tune of the last bunch and the vertical tune of the first bunch in a train, which should both be lower. However, more recent tune data for all pbar bunches, taken in a successor experiment on 12/03, suggest that the bunch A24, at the end of a train, which is displayed in the control room might actually correspond to A13 in the theoretical description. If this turns out to be the case, the lower vertical tune observed in the present experiment would be consistent with the expectation. The vertical tunes of the other pbar bunches would then be expected to be similar to, or even slightly higher than, those of the protons, and the tune difference between A24 and the protons could almost entirely be attributed to the long-range beam-beam collisions.

After pbar removal the proton chromaticities were measured for the collision optics at 980 GeV, with the result Ch=13 and Cv=16.

A significant discrepancy was seen between FBIANG and SBDAIS readings for pbars at low intensity. The numbers from SBDAIS seem to be more consistent with the observations on flying wires and synchrotron-light monitor.

The emittance inferred from the synchrotron light monitor was low by about a factor of 2 compared with the flying

wire emittance. This discrepancy persisted down to fairly low intensities.

Extracting the beam size directly from the beam loss during the scraping will require a simplified experiment, where only a single collimator jaw is moved into the beam.

REFERENCES

[1] P. Bagley, `Beam Beam Tune Shifts for 36 Bunch Operation in the Tevatron', EPAC'96, Sitges (1996).